

Characterization of DhHal3p: A moderately thermostable FMN-Binding Flavoprotein with biomedical potential from halotolerant yeast, *Debaryomyces hansenii* using partial structure prediction

Aditi Sharma^{1#,*}, Rashmi Singh^{1#,*}, Arzoo Kumari², Sanjeev Puri¹, Shailendra Kumar Arya¹, Ruchi Sachdeva² & Anu Priya Minhas^{1,3*}

¹Department of Biotechnology, University Institute of Engineering and Technology, Panjab University, Chandigarh-160 014, India

²Department of Bioinformatics, Goswami Ganesh Dutta Sanatan Dharma College, Panjab University, Chandigarh-160 030, India

³Biological Sciences, National Institute of Occupational Health (ICMR-NIOH), Ahmedabad-380 016, Gujarat, India

Received 26 July 2023; revised 26 April 2024

Enzymes within the CoA biosynthetic pathway are highlighted in the literature as promising targets for antimicrobial drugs, beyond their role in metabolism. In *Saccharomyces cerevisiae*, the model yeast, the Hal3 protein is a pivotal component of the PPCDC complex, a critical enzyme involved in the fourth step of Coenzyme A (CoA) biosynthetic pathway. Characterizing such proteins from extremophilic strains might present their substantial therapeutic potential. Therefore, the focus of the present study was to identify and characterize the putative *DhHal3* gene and encoded protein from *Debaryomyces hansenii*, a halotolerant and teleomorph of commensal yeast, *Candida famata*. *DhHal3* encoded a 559 amino acids peptide with a unique 48 amino acids aspartic acid-rich C-terminal domain. DhHal3p was identified as a flavoprotein (PFAM ID "PF02441") with conserved PLXANT and PXMNXMW motifs, and H³⁴⁴ residue involved in FMN binding. Heterogeneously expressed 6xHistidine-tagged DhHal3p appeared as ~73.37kDa protein on SDS-PAGE, exhibiting pyruvate decarboxylation activity ($V_0 = 0.57$ units/mL) *in vitro*. Thermo-profiling and circular dichroism (CD) analysis suggested DhHal3p is a moderately thermostable FMN-binding flavoprotein from *D. hansenii*. Docking simulations supported strong interactions between DhHal3p structure and FMN (binding energy = -4.04 kcal/mol). Further investigation into the functional characteristics of DhHal3p could yield pivotal insights into a variety of cellular processes, paving the way for therapeutic interventions.

Keywords: *Debaryomyces hansenii*, Decarboxylase, Docking, Flavoprotein, PPCDC, DhHal3p

Phosphopantothencysteine decarboxylase (PPCDC) enzyme complex is a crucial component of the Coenzyme A (CoA) biosynthetic pathway, responsible for catalyzing the fourth step of the pathway and has been identified as the novel antimicrobial drug targets^{1,7}. *Hal3*-encoded flavoprotein is a key component of the PPCDC enzyme complex. Unlike homo-dimeric PPCDC in humans and plants, *Saccharomyces cerevisiae*, the moderately halotolerant

model yeast, PPCDC is a heterotrimer made up of three different subunits - Vhs3, Hal3, and Cab3²⁻⁵. Hal3p is a regulatory subunit, to the catalytic Vhs3 subunit and Cab3, responsible for stabilizing the Hal3-Vhs3 interaction and overall stability of the PPCDC complex. Hal3 shares 63% and 37% sequence identity with Vhs3 and Cab3, respectively. Understanding the molecular mechanisms of the PPCDC complex in yeast may have implications for the development of new therapeutic strategies for various diseases related to CoA metabolism^{1,6}. Other than PPCDC activity, Hal3 has also been identified as a multifaceted protein with diverse functions, naming it as moonlighting flavoprotein. The diversification in Hal3-associated phenotypes is a result of its partnership with a downstream protein phosphatase, Ppz1, resulting in the alteration in the expression of various transporters and proteins such as Na⁺ ATPase, high-affinity potassium transporters (Trk1/Trk2),

*Correspondence:

#Both the authors are contributed equally

E-mail: anu.minhas@icmr.gov.in, annuminhas@gmail.com (APM); aditisharma102@gmail.com (AS); rashmisingh.singh60@gmail.com (RS)

Abbreviations: CD, circular dichroism; FMN, Flavin mononucleotide; Kb, kilobases;kcal, kilocalories;kDa, kilo Dalton; nt, nucleotide; PDC, Pyruvate decarboxylase; PPCDC, Phosphopantothencysteine decarboxylase; p, protein;SDS-PAGE, Sodium dodecyl-sulfate polyacrylamide gel electrophoresis

Suppl. Data available on respective page of NOPR

kinase (Mapk1), and cyclins⁷⁻⁹. Surprisingly, Ppz1 has been reported only in fungi^{10,11}.

Debaryomyces hansenii is a hemiascomycetous, heterogeneous, nonconventional, euryhaline, and antagonistic yeast, with the ability to catabolize a wide range of carbon sources. Recently, *D. hansenii* in the human gut mycobiome, was found to modulate human immune response. Studies on the gut mycobiome suggest a negative correlation between the presence of *D. hansenii* and *Candida* in the human gut^{1,3}. Additionally, *D. hansenii* has been found to produce killer toxins (mycocins) that are effective against opportunistic pathogenic *Candida* and other human pathogenic fungi^{12,13}. Unfortunately, due to limited molecular tools available for its genome alteration, only a small number of genes and proteins have been well-characterized in *D. hansenii* so far¹⁴⁻¹⁶.

The main objective of this study was to identify and characterize the *DhHal3* gene and its corresponding protein, DhHal3p from *D. hansenii* CBS767. To achieve this goal, a multifaceted approach was utilized, integrating computational methods such as genome mining, protein structural modeling, and docking studies with molecular methods for isolating and characterizing *DhHal3* and DhHal3p. Additionally, *in vitro* experiments were conducted involving the expression, purification, and biochemical evaluation of His-tagged DhHal3p to validate the above findings.

Materials and Methods

Strains and reagents

The yeast strain *D. hansenii* CBS767 (MTCC 3461) and bacterial strains (*E. coli* DH10 β and BL21) used in this study were kindly received from Dr. Alok Mondal of IMTECH, Chandigarh, while pET43a was a kind gift from Dr. Ajay Pandey of NABI Mohali. YPD, LB media, and antibiotics used in this study were purchased from Himedia. IPTG, protease inhibitor cocktail, and PMSF were obtained from Sigma Aldrich, and Ni-NTA slurry was purchased from Qiagen. All DNA modifying enzymes used in this study were purchased from New England Biolabs, UK.

Isolation of putative *DhHal3* homolog from *D. hansenii*

To retrieve *Hal3* homolog from *D. hansenii* genome, the protein sequence of ScHal3 from *S. cerevisiae* (baker's yeast) with accession number AAA80000¹⁷ was used as a query sequence for tBLASTn against the *D. hansenii* CBS767 (taxid:284592)

(<https://blast.ncbi.nlm.nih.gov/blast/Blast.cgi>) program at NCBI. Further physicochemical characteristics such as pI and molecular weight were estimated using protein sequence by using the ExPasy proteomic server (<https://web.expasy.org/translate/>)¹⁸ ClustalW analysis between similar flavoproteins was performed.

In silico identification of fungal flavoproteins

The flavoprotein's PFAM ID obtained from the InterProScan database was used to search fungal flavoproteins on the Ensembl Fungi database (<https://fungi.ensembl.org/index.html>)¹⁹. Of the obtained fungal flavoproteins, subsequent analysis was carried out only with flavoproteins characterized as PPCDC. Translated DhHal3p was included as the query sequence. Protein architecture analysis of the selected flavoprotein sequences was performed using Multiple Em (Expectation maximization) for Motif Elicitation (MEME) program version 5.0.5 (meme-suite.org)²⁰. Further, MEGAX software by the Neighbor-joining method was used for phylogenetic analysis²¹ and Blast2GO for functional annotation. Further, the same Pfam ID was used to retrieve all flavoproteins from *D. hansenii* genome.

Retrieval of ligands, FMN and Pyruvate

PubChem (<https://pubchem.ncbi.nlm.nih.gov/>) is an accessible repository of experimental data for small molecule's biological activity and chemical structures. The purpose of PubChem is to make this data easily available to biological researchers. PubChem provides services that offer tools for the quick retrieval of data²². The compound FMN (Flavin mononucleotide) (PubChem CID:-643976) and Pyruvate (PubChem CID:-107735) are downloaded from PubChem in SDF format and then converted into PDB format using Pymol for further Docking process.

PPCDC protein model building

Modeller (<https://salilab.org/modeller/>) was used to predict the tertiary structure of the protein PPCDC (Phosphopantothencycysteine decarboxylase complex) (Uniprot ID: A0A1B1SK43; Sequence length: 559 amino acids). It is a computer program for automated protein homology or comparative modeling. In the most basic case, the input consists of an alignment of a sequence to be modeled with the template structures, the template's atomic coordinates, and a simple script file. MODELLER then calculates a model comprising all non-hydrogen

atoms automatically in min^{23} . BLAST (Basic Local Alignment Search Tool) was used to find suitable templates with sequence identity of more than 30% of the query sequence against PDB (Protein Data Bank) ²⁴.

Energy minimization

Yasara (Yet another Scientific Artificial Reality Application) (http://www.yasara.org/minimization_server.htm) energy minimization server uses the Yasara force field to minimize the energy of a protein model. The server accepts the PDB format of the protein structure as input. The SCWRL algorithm is used to predict the best amino acid side-chain rotamers, and the YASARA force field with implicit solvent is used to optimize the rotamers in dihedral angle space using steepest-descent minimization. Then, to remove any remaining clashes, a steepest descent minimization is applied, followed by a simulated annealing minimization to achieve a stable nearby conformation having minimum energy. The minimization process stops after 200 steps ²⁵.

Avogadro (<https://avogadro.cc/>) is molecule editor and visualization software for computational chemistry, molecular modeling, materials science, bioinformatics, and related fields. Avogadro also provides a platform for geometry optimization of small molecules. For ligand optimization, the UFF (universal force field) and 500 steps of steepest descent algorithm were applied first, followed by 500 steps of conjugate gradient algorithm ²⁶.

Docking

AutoDock (<https://autodock.scripps.edu/>) is a set of automated docking tools. It was developed to anticipate the interactions of small compounds, such as drug candidates or peptides, with a protein's known tertiary structure. Two software generations are currently provided for AutoDock: AutoDock 4 and AutoDock Vina. For the docking of our protein and ligand, we used AutoDock 4. The two major programmes in AutoDock 4 are autodock and autogrid. Autodock 4 docks the ligand to a set of grids that describe the target protein, while autogrid pre-calculates these grids for atoms internally. A semiempirical free energy force field is used by AutoDock 4 to predict the binding free energies of small ligands to macromolecular targets. Autodock provides graphical user interface (GUI) to analyze docking results ²⁷. Docking is carried out using Lamarckian genetic algorithm (LGA) with default parameters (number of GA runs: 10, population size:

150, maximum number of evaluations: 2,500,000, maximum number of generations: 27,000, rate of gene mutation: 0.02, rate of cross over: 0.8). The grid size for docking was 112, 120, and 96 along the X, Y, and Z axis respectively with 0.375Å spacing. The grid is defined using PyMol by visualizing the reference protein-ligand interaction in this case the protein PPCDC, AtHAL3a [*A. thaliana*] (PDB ID: - 1e20) and ligand FMN. The docking complex with the lowest binding energy was selected out of the ten conformations. Also using LGA with the default parameters protein (PPC decarboxylase complex) and ligand (pyruvate) are docked with the grid size of 74, 72, 60 along X, Y, and Z axis, respectively, and spacing of 0.375Å. Further, the docking complexes were analysed using Discovery Studio.

DhHal3 isolation and cloning

Genomic DNA from *D. hansenii* CBS767 was isolated following standard protocol ²⁸. *DhHal3*-specific PCR primers were designed using Gene Runner software. PCR was carried out using *pfu* DNA polymerase (New England Biolabs), Hal₃OrfpetF (5'-CGAGCTCACATGGTTTCAGAAAATGGTGCT-3') and Hal₃OrfpetR (5'-CCCAAGCTTTTAAGTGTTATTAGATTCTTCTCTTCA-3') primer pair at 49°C annealing temperature for 30 cycles. To isolate *DhHal3* from *D. hansenii*, *DhHal3* PCR products were cloned in pJET 1.2 vector to obtain pJH1 plasmid at complementary enzyme sites. Plasmid isolation was performed following the alkaline lysis method as described previously (Sambrook and Russell, 2001). Further, to express 6xHis tagged DhHal3p, pDHA2 plasmid was constructed using IPTG inducible Lac promoter. For this, the *DhHal3* PCR fragment was amplified using the genomic DNA of CBS767 as a template using the same primer pair. SacI-HindIII digested PCR fragment was cloned at the complementary site in pET43a to obtain pDHA2. Cloning was confirmed by restriction digestion, colony PCR and DNA sequencing (Scigenome, Bangalore).

Expression and purification of recombinant 6x Histidine tagged DhHal3p

To express DhHal3p, pDHA2 was transformed into BL21 (DE3) strain using the standard calcium chloride method of transformation ²⁹. Selected transformants were grown at 37°C and induced with 0.2 mM IPTG at A600 ~0.4-0.6. Initially, induction was carried out at 16°C, 28°C, and 37°C for 10 h, followed by cell harvest, cell pellets resuspension and

sonication in lysis buffer (Tris-HCl (pH 7.5), NaCl, PMSF, protease inhibitor). For final purification, 6xHis tagged DhHal3p induced at 16°C for 16 h was subsequently purified using Ni-NTA affinity agarose beads following the manufacturer's instructions (Qiagen, Germany). Briefly, loading a mixture of lysate and Ni-NTA affinity agarose beads (Qiagen) onto the equilibrated column with 1 h incubation at 4°C following three washes, the bound protein was eluted in elution buffer (Tris NaCl buffer:pH 8.0, 30 mM imidazole). Protein quantification was carried out using Bradford estimation (Himedia) and the BSA standard curve. The eluted protein was stored at -70°C until use. Protein visualization involved running 8% SDS-PAGE at 120 V for 60 min using a Mini Protean II system (BioRad, Hercules, CA, USA). Additionally, 8% native gel was also run.

CD analysis

To find the role of FMN in DhHal3 structural integrity, Holo-and Apo-DhHal3p (referring to FMN bound and unbound respectively) were prepared as per³⁰ and subjected to CD analysis. In brief, ~5 mg of purified DhHal3p was incubated at 4°C for 1 h with equilibrated Ni-NTA slurry. NTA-bound DhHal3p was extensively washed with 10 volumes of buffer containing 2 M urea and 2 M KBr to remove the protein-bound FMN. The column was washed twice with 10 volumes of 50 mM phosphate buffer (pH 8.0) and de-flavinated Apo-DhHal3 was eluted with 30 mM imidazole. To generate Holo-DhHal3, FMN reconstitution was done by incubating column-bound Apo-DhHal3 with 10 mM FMN at 4°C overnight. The obtained Holo-and Apo-DhHal3p were subjected to CD analysis separately. Far-UV CD spectra were recorded using a J-810 CD spectro polarimeter (JASCO, Japan) using wavelength scan between 190-400 nm at RT using filtered pure protein (0.2 mg/mL). The resolution was set as 0.2 nm and the path length was set as 0.1 cm.

Enzymatic activity

The decarboxylase activity of recombinant DhHal3p was assessed as described in Gounaris *et al.*'s (1971) standard pyruvate decarboxylase assay³¹. Pyruvate decarboxylase catalyses the decarboxylation of pyruvate to acetaldehyde and carbon dioxide, and β -NADH is oxidized to β -NAD⁺ during the reaction. The amount of β -NADH consumed or the amount of β -NAD⁺ produced by the reaction can be measured spectrophotometrically. The change in the absorbance at A₃₄₀ is proportional to the amount of β -NADH

consumed, which is subsequently related to the activity of the pyruvate decarboxylase enzyme in the sample. The assay involved meticulous monitoring of the β -NADH to β -NAD conversion over 5 min at pH 6.0 and 25°C. The reaction mixture comprised 2.7 mL of 200 mM citrate buffer (pH 6.0), 100 μ L of 1.0 M sodium pyruvate, 50 μ L of 6.4 mM β -NADH, and 50 μ L of ADH. Following the addition of 100 μ L of enzyme, the reaction volume was adjusted to 3.0 mL (standard assay condition). The activity was expressed in units/mL, defined as the quantum of activity required to transform 1.0 μ mol of pyruvate to acetaldehyde per minute.

Thermo and pH profiling

The effect of temperature on DhHal3p activity was assessed by pre-treating protein at 20°C to 80°C for 5 min followed by assay as described above. The activity was measured by plotting an absorbance vs time graph. The effect of pH was analysed by performing the same assay with buffers pH ranging from 2.0 to 14.0. The buffer pH was adjusted with 0.5M citric acid for pH 2.0-4.0, 0.5 M sodium acetate for maintaining pH 4.0-6.0, 0.5 M sodium phosphate for pH 6.0-8.0, 0.5 M Tris-HCl for pH 8.0-9.0 and 0.5 M glycine-NaOH for pH 9.0-14.0. Further, an absorbance vs time graph was plotted and compared to a graph at pH 6.0.

Results and Discussion

Identification, isolation and cloning of putative DhHal3 homolog

Through a comprehensive genome mining approach, employing *S. cerevisiae* ScHal3 protein sequence as a query from *Saccharomyces* Genome Database (SGD) and tBLASTn (<http://blast.ncbi.nlm.nih.gov/blast/Blast.cgi>), a 1677 nt sequence corresponding to the putative *hal3* gene ortholog was successfully identified. The identified *hal3* was found to be present on chromosome D (GenBank accession no. CR382136.2) in the *D. hansenii* genome, spanning from coordinates 1344271-1345950. The putative DhHal3 was translated into a 559 amino acid-long peptide, shared 46.04% identity with the *hal3* homolog from *S. cerevisiae*¹⁷ and harboured a unique 48 amino acid long C-terminal tail rich in aspartic acid (D). tBLASTn analysis using translated *hal3* sequence verified it as the putative DhHal3 gene from *D. hansenii*.

Furthermore, flavoprotein PFAM ID "PF02441" obtained from the InterPro database (<https://www.ebi>

ac.uk/interpro/result/InterProScan) was used for analysing fungal flavoproteins available with the Ensemble database. This search yielded a total of 3587 sequences, encompassing hypothetical as well as well-characterized fungal flavoproteins. Of these, 156 flavoproteins with PPCDC activity were selected for subsequent analysis (Table S1). Phylogenetic analysis revealed these 157 fungal flavoproteins belonged to four major clusters, cluster I comprised 98 flavoproteins (Red), cluster II comprised 32 flavoproteins (Yellow), cluster III comprised 26 flavoproteins (Green) while cluster IV with only 1 flavoprotein (Blue). *DhHal3* was located in cluster II, next to *S. cerevisiae* (Fig. 1). Motif analysis revealed five conserved motifs *i.e.*, motif 1, motif 2, motif 3,

motif 4 and motif 5 among 111 flavoproteins (Fig. 2A). However, *DhHal3p* had only four motifs (1, 2, 3 and 5) (Fig. 2B).

The Ensembl Fungi analysis revealed four genes encoding flavoproteins within *D. hansenii* genome. These genes were identified as CAB3, PAD1, VHS3, and SIS2/HAL3. SIS2/HAL3 (Gene ID: DEHA2D16082g, 559 amino acids) was found to be located at chromosome D as indicated above, while CAB3 (Gene ID: DEHA2D16082 g, 559 amino acids), PAD1 (Gene ID: DEHA2D16082 g, 559 amino acids), VHS3 (Gene ID: DEHA2D16082 g, 559 amino acid) were present on chromosomes E, G and G, respectively. In *S. cerevisiae*, Hal3p (regulatory subunit), Vhs3 (catalytic subunit) and Cab3 are parts

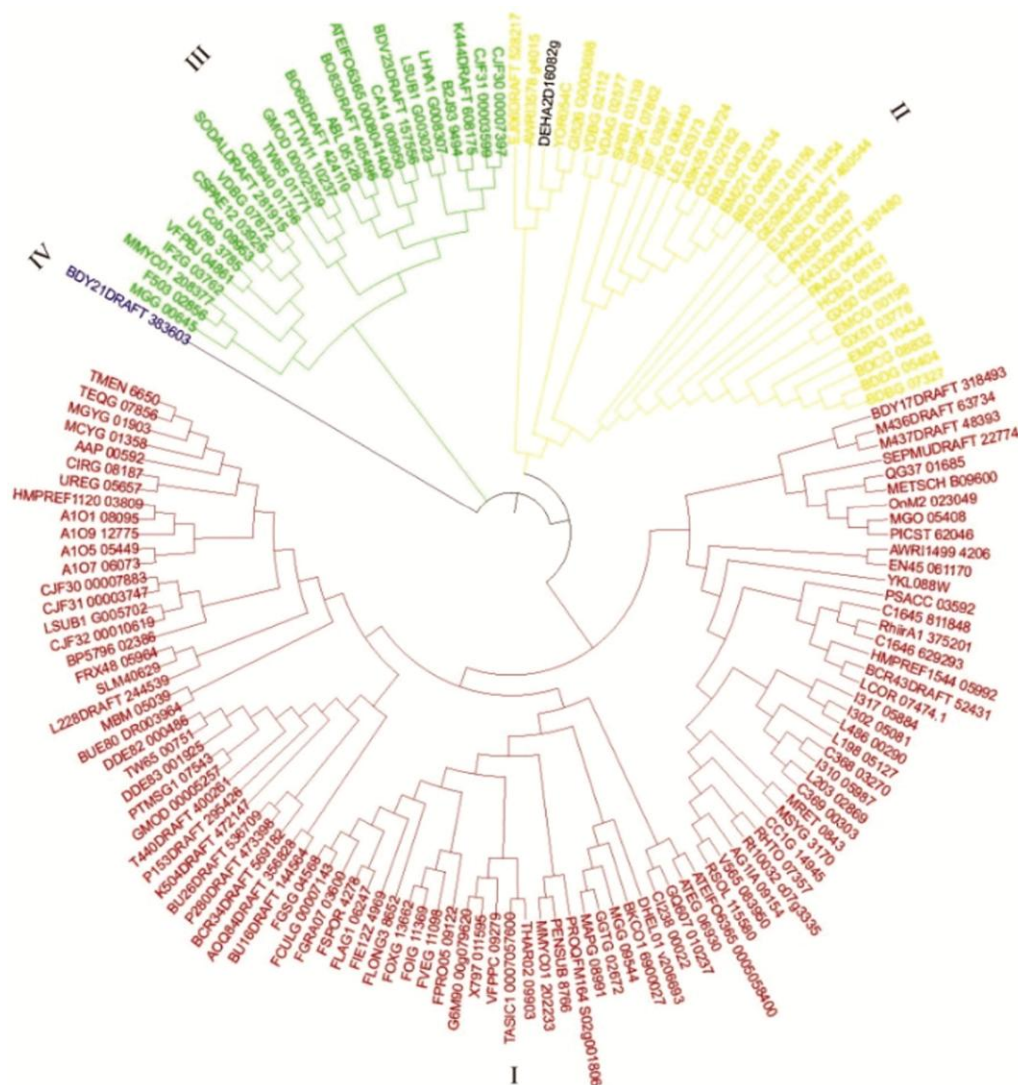


Fig. 1 — Phylogenetic analysis of 157 fungal flavoproteins by Neighbour joining method. Phylogenetic tree showed Cluster I contained 98 (Red), cluster II contained 32 (Yellow), cluster III contained 26 flavoproteins (Green) while cluster IV only contained 1 flavoprotein (Blue). *DhHal3* from *D. hansenii* could be located in cluster II, close to *S. cerevisiae*

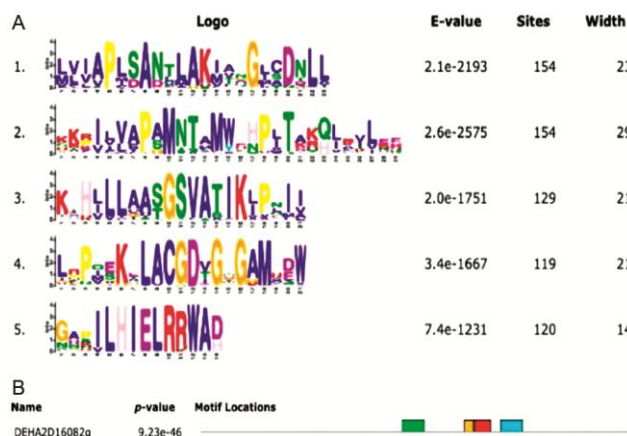


Fig. 2 — Motif analysis of 156 fungal flavoproteins. (A) 111 flavoproteins have five common motifs *i.e.*, motif 1, motif 2, motif 3, motif 4 and motif 5; and (B) DhHal3p from *D. hansenii* showed only four (1, 2, 3 and 5) out of five motifs. Motif 4 was missing in DhHal3p

of the PPCDC complex sharing 63% and 37% sequence identity with Vhs3 and Cab3, respectively^{1,6} (Fig. 3A & B).

The co-factor flavin mononucleotide (FMN) serves as a critical component in redox reactions, playing a pivotal role in the generation of 4'-phosphopantetheine, EpiD, and Dfp flavoproteins^{2,32-35}. ClustalW analysis revealed the presence of PLXANT and PXMNXXMW conserved motifs among Hal3 orthologs (ScHal3p, AtHal3p and DhHal3p) from *S. cerevisiae*, *Arabidopsis* and *D. hansenii*, respectively (Fig. 4). In AtHal3a ortholog, His⁹⁰, Cys¹⁷⁵ and Asn¹⁴¹ residues (in motif 5, 4 and 2, respectively) are required for FMN binding⁵. DhHal3p sequence also showed conserved histidine and Asn residue, as H³⁴⁴ and in PXMNXXMW motif, respectively, required for FMN binding revealing DhHal3p, a flavoprotein.

DhHal3 cloning

The DNA sequencing analysis of clones, pJH1#1 and pJH1#2 (Fig. 5A), containing *DhHal3* ORF *D. hansenii* was deposited in the NCBI database under the accession number KX196448 gene (~1.67 kb) (Fig. 5B), confirmed the integrity of the cloned *DhHal3* PCR fragment. This study was the first study on isolation and cloning of the *DhHal3* open reading frame (ORF) from *D. hansenii*. The comprehensive analysis revealed intriguing features intrinsically in DhHal3p flavoprotein. DhHal3p consisted of 559 amino acids and exhibited a remarkable characteristic unique 48 amino acids aspartic acid (D) -rich C-terminal tail. The predicted isoelectric point (pI) of

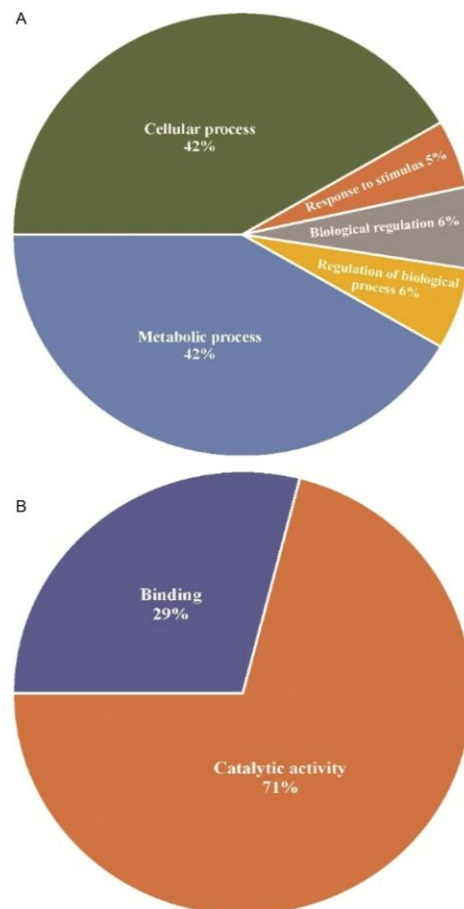


Fig. 3 — Blast2Go annotation gene ontology (GO) mapping of these fungal proteins. (A) Functional annotation of 156 flavoproteins in biological process. The graph shows 6% of proteins involved in biological regulation, 5% response to stimulus, 42% cellular responses, 6% regulation of biological processes, and 42% metabolic processes; and (B) The molecular functional analysis of 156 flavoproteins revealed 29% of proteins involved in binding and 71% in catalytic activity

DhHal3p was 4.32, with 61,660 Dalton molecular mass. In contrast, the C-terminal tail of Hal3 in *S. cerevisiae*, the moderately halotolerant yeast is comparatively shorter, spanning only 28 amino acids. This discrepancy underscores the distinctive nature of DhHal3p in comparison to its counterpart in *S. cerevisiae*.

DhHal3p expression, purification and biochemical characterization

To obtain the 6xHis tagged DhHal3p protein, the clone pDHA2#B4 (as shown in Fig. 5C above), containing *DhHal3* gene under the IPTG-inducible lac promoter, was heterogeneously expressed in the bacterial host *E. coli* BL21 (DE3). The soluble lysates of the bacterial cells demonstrated the presence of the 6xHis tagged DhHal3p protein at all induction temperatures,

in a final protein concentration of $\sim 15 \mu\text{g/mL}$, was used. These results provide valuable evidence of the decarboxylation capability of DhHal3p and support its potential role within the PPCDC complex.

DhHal3p could also reported to retain its decarboxylation activity (100%) when pre-treated at temperature 50°C and below for five min each (Fig. 7A) below. Nevertheless, DhHal3p activity rapidly declined to 20% when protein was pre-treated at and above 60°C . These results indicated that DhHal3p from *D. hansenii* is a cytoplasmic, moderately thermostable flavoprotein exhibiting limiting PDC activity. Regarding pH profiling, oxidation of $\beta\text{-NADH}$ to $\beta\text{-NAD}$ indicated DhHal3p was able to decarboxylate pyruvate under acidic and neutral pH range (pH 2-6). However, a sharp decrease in the activity (up to 80%) was reported beyond pH 6. The activities were calculated as relative percentages to the activity at pH 6 (Fig. 7B) below. Similar pH optima of 5.8 and 6.0 have been reported for PDC isolated from *S. cerevisiae* and *Kluyveromyces pastoris*, respectively³⁶. Further investigation is required to understand the sudden drop in activity observed for DhHal3p at pH 8.0 and above. This could involve examining the pH stability profiles of all reaction components and intermediates before drawing definitive conclusions.

Subsequently, to validate the role of FMN in DhHal3p structural integrity, far-UV CD spectra of purified and dialyzed DhHal3p were obtained (Fig. 8A). CD spectroscopy is a sensitive technique to monitor the conformational changes of proteins as well as great importance for the structural folding and binding properties of proteins. Proteins with well-defined antiparallel β -pleated sheets have positive bands at 195 nm and negative bands at 218 nm, while the disordered protein structures display low ellipticity above 210 nm and negative bands near 195 nm³⁷. Far-UV CD spectra of purified and dialyzed DhHal3p showed the presence of α -helix, β -pleated sheets and random turns as indicated by characteristic spectra obtained between 190-195 nm and 208-222 nm (Fig. 8B below). Far-UV CD spectra of purified Apo-DhHal3p also showed the positive band at 190-195 nm and a negative peak at around 217 nm, indicative of characteristic α -helix. A small shift in mean residue ellipticity ($\text{degree cm}^2 \text{dmol}^{-1}$) in CD spectra from θ_{-60} to θ_{-100} and in the region >230 nm indicated a change in global protein conformation in the presence of FMN (Fig. 8C).

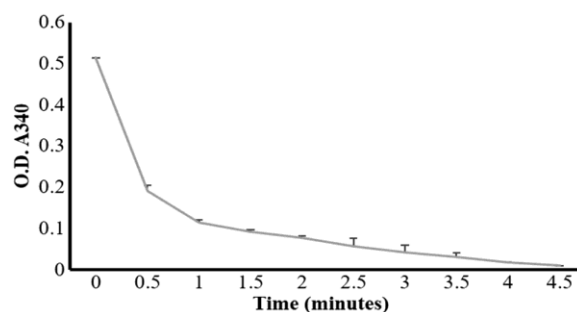


Fig. 6 — Pyruvate decarboxylase activity (PDC) graph. DhHal3p was assessed for PDC activity as described in Gounaris *et al.* (1971) standard decarboxylase assay (40). The change in the absorbance at A_{340} is proportional to the amount of $\beta\text{-NADH}$ consumed, which is subsequently related to the activity of the pyruvate decarboxylase enzyme in the sample. The activity was expressed in units/mL, defined as the quantum of activity required to transform $1 \mu\text{mol}$ of pyruvate to acetaldehyde per minute

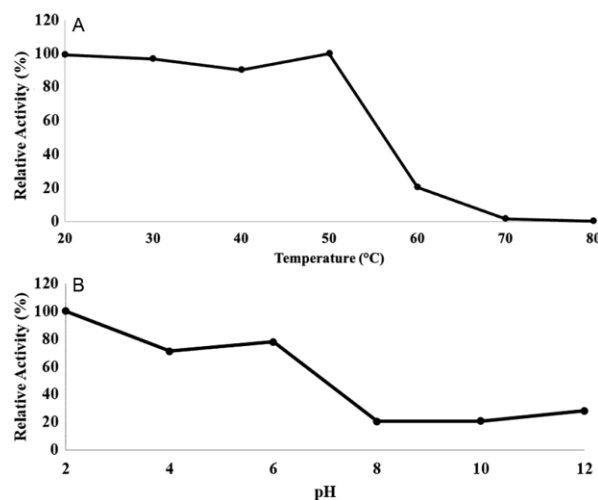


Fig. 7 — (A) Effect of temperature on the enzymatic activity of DhHal3p. DhHal3p retained its activity when pre-incubated to 50°C for five min. However, DhHal3p activity rapidly declined and retained only 20% when pre-incubated at 60°C and above; and (B) Effect of pH on the enzymatic activity of DhHal3p. DhHal3p was able to decarboxylate pyruvate under the acidic and neutral pH range (pH 2-6). However, a sharp decrease in the activity (almost 80%) was reported beyond pH 6. The relative activity is calculated as the percentage of activity at standard conditions of pH and temperature

These results indicated that DhHal3p is a flavoprotein with FMN playing a crucial role in DhHal3p structural integrity and is comparable with docking results (mentioned below). The role of FMN in preserving the Hal3 trimer structure has also already been reported in rice and *Arabidopsis* Hal3p². In future, the role of FMN in DhHal3p enzymatic activity and the effect of other cofactors need to be investigated.

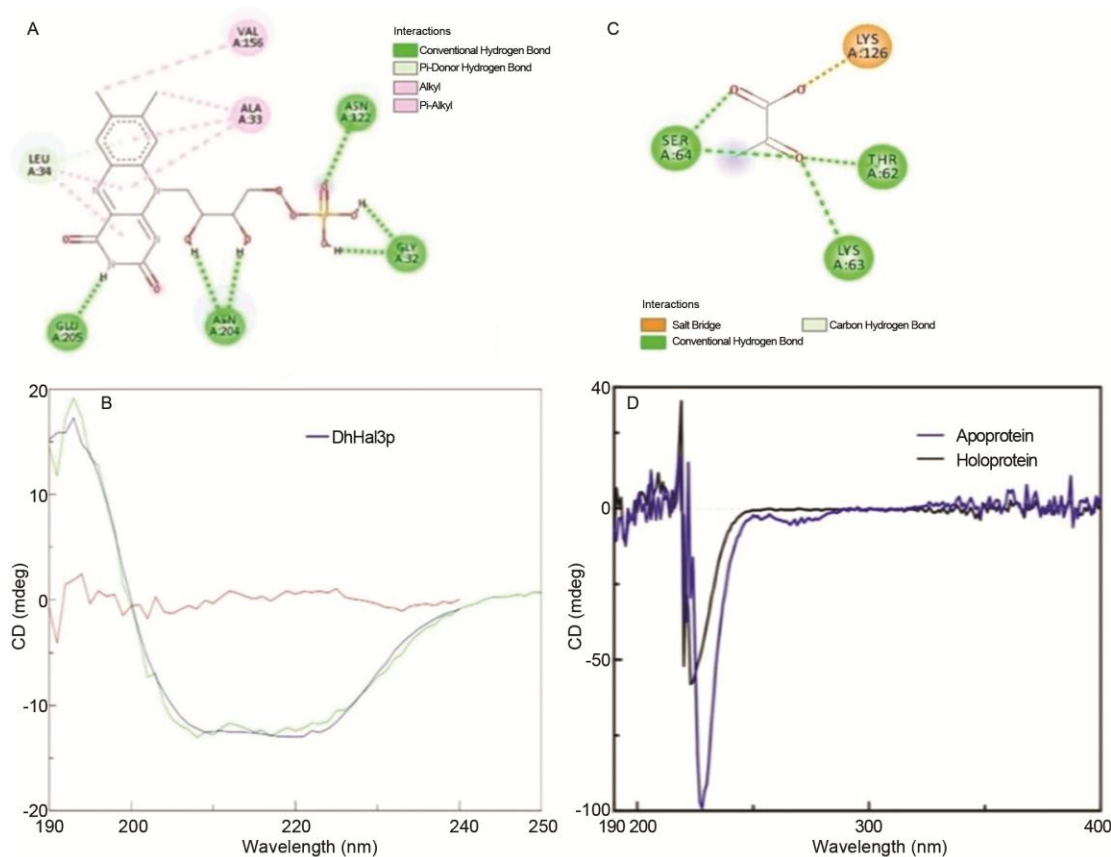


Fig. 8 — (A) Protein-ligand docking analysis showed 4 hydrogen bonds form between DhHal3p and ligand FMN. The ligand FMN formed hydrogen bonds with residues GLY32 (272), ASN122 (362), ASN204 (444), and GLU205 (445) (number in bracket represents original positions of respective residue in DhHal3p sequence) of DhHal3p; (B) Far-UV CD spectra of purified and dialyzed DhHal3p; (C) Far-UV and near-UV spectrum of Apo-DhHal3p (blue colour) and Holo-DhHal3p (black colour); and (D) Docking analysis using pyruvate as a ligand, it was found that DhHal3p formed three hydrogen bonds with THR62 (302), SER64 (304), and LYS126 (366) residues (number in bracket representing original positions of respective residue in DhHal3p sequence)

DhHal3p Tertiary model prediction

To investigate the interaction of DhHal3p with FMN and pyruvate, tertiary structure prediction of putative Phosphopantothencysteine decarboxylase (DhHal3p) was performed using homology modelling. When a query protein shares a sequence similarity with a protein whose atomic structure is known, homology modelling is the most effective technique for predicting the tertiary structure of proteins. For DhHal3p, only single template Phosphopantothencysteine decarboxylase also called FMN binding protein AtHal3 (PDB ID: 1E20; Resolution: 2.02Å) from *Arabidopsis thaliana* with 34% query coverage, 38.27% sequence identity and 1e-38 e-value against target protein was available. *Arabidopsis thaliana* flavoprotein AtHAL3 catalyzes a crucial Step in the biosynthesis of Coenzyme A by

decarboxylation of 4'-Phosphopantothencysteine to 4'-Phosphopantetheine. Plant growth, as well as salt and osmotic tolerance, is related to the *Arabidopsis thaliana* flavoprotein AtHAL3³. Only the C-terminal domain region of the target protein (DhHal3p) was aligned with the template protein (AtHAL3), so only the C-terminal region of the template protein was modeled. Twenty homology models of the query protein were obtained using Modeller and selected the best model having a DOPE score of -18799.49805^{23,38}.

Energy minimization

For the structure built from Modeller, energy minimization was performed using the YASARA server. The structure obtained after minimization had less energy (-412831.1 KJ/mol) than the structure before minimization (Table 1 below).

So the protein structure after minimization is more stable than before²⁵. The ligands retrieved from PubChem were also minimized using the Avogadro tool and had lower energies after the minimization process than before (Table 2 below).

Following protein minimization, we created a Ramachandran plot of the *DhHal3* protein using Procheck. The Ramachandran plot showed that 77.7% of the residues are in the most favoured regions, 18.5% residues in the additional allowed regions, 3.1% residues in the generously allowed regions, and 0.7% residues in the disallowed region (Fig. 9).

DhHal3p docking with FMN and Pyruvate

A computational docking approach was used to scrutinize the structural dynamics of the DhHal3p-FMN (flavin mononucleotide) complex, providing a detailed examination of the spatial arrangement and molecular interactions between DhHal3p and its cofactor and shedding light on their functional relationship. Protein-ligand docking analysis showed the formation of four hydrogen bonds between

DhHal3p and ligand FMN. FMN formed hydrogen bonds with DhHal3p via its GLY32 (272), ASN122 (362), ASN204 (444), and GLU205 (445) (number in bracket represents original positions of respective residue in DhHal3p sequence) as shown in (Fig. 8A) above compared to His⁹⁰, Cys¹⁷⁵ and Asn¹⁴¹ residues in AtHal3a ortholog⁵. The docking interaction between DhHal3p and FMN exhibited a binding energy of -4.04 kcal/mol, suggesting a strong affinity between the two entities as evident³⁰⁻⁴¹.

Next, docking analysis between pyruvate and DhHal3p homology model (partial) showed DhHal3p forming three hydrogen bonds with THR62 (302), SER64 (304), and LYS126 (366) residues (number in bracket represents original positions of respective residue in DhHal3p sequence) (refer to Fig. 8D above) with 2.46 kcal/mol binding energy, indicating a weaker affinity. The limited availability of the entire structure of DhHal3p in the computational part may have constrained its interaction with pyruvate since only the C-terminal half was modeled. Before drawing a definitive conclusion regarding the enzymatic specificity of DhHal3p towards pyruvate, it is crucial to have a thorough understanding of the oligomeric form of DhHal3p. In most eukaryotes, including *A. thaliana*, PPCDC is a homo-oligomeric flavin-containing Cys decarboxylases (HFCD) protein family member and AtHal3ap catalyzes the decarboxylation of (R) -4'-phospho-N-pantothoenylcysteine to 4'-phosphopantetheine. Exception to this, *S. cerevisiae*, Hal3p (ScHal3) in its monomeric state, regulates the Ser/Thr protein phosphatase Ppz1 and joins Cab3 and Hal3 paralog, Vhs3 to form a heterotrimeric PPCDC enzyme catalyzes the decarboxylation step in CoA biosynthesis pathway^{3,42}.

Conclusion

This study represented the first investigation into the isolation, cloning, and characterization of *DhHal3* and its protein counterpart from *D. hansenii*, a halotolerant model yeast. The *DhHal3* gene was 1677 nucleotides long. Translated DhHal3p was 559 amino acids in length, shared 46.04% identity with the hal3 homolog from *S. cerevisiae*¹⁷ but had a distinct long C-terminal tail compared to its shorter counterpart in *S. cerevisiae*. DhHal3p contained four conserved motifs specific to flavoproteins. Through bioinformatic analysis, docking studies, and subsequent CD and enzymatic assessments, it was strongly indicated that *DhHal3* serves as a moderately

Protein	Energy before minimization (KJ/mol)	Energy after minimization (KJ/mol)
DhHal3p	-143181.4	-412831.1

Ligand	Energy before minimization (KJ/mol)	Energy after minimization (KJ/mol)
FMN	-536.721	-589.872
Pyruvate	346.55	337.726

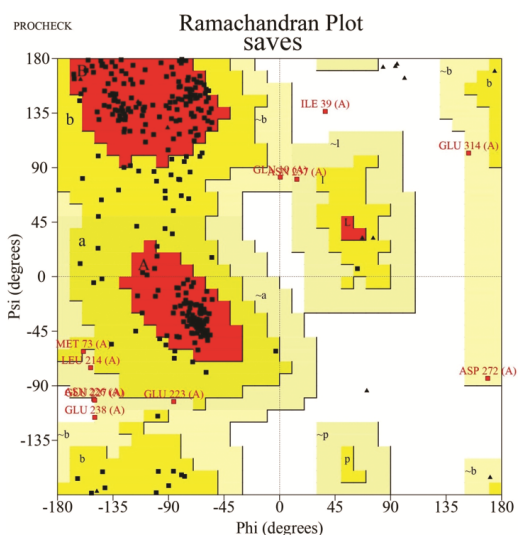


Fig. 9 — The Ramachandran plot showed that 77.7% of the residues are in the most favoured regions, 18.5% residues in the additional allowed regions, 3.1% residues in the generously allowed regions, and 0.7% residues in the disallowed region

thermostable FMN-binding flavoprotein from *D. hansenii*, displaying pyruvate decarboxylase activity.

Hal3 is a crucial component of PPCDC, an integral part of CoA enzyme biosynthetic pathway and therefore Hal3 characterization might serve as a foundational discovery, paving the way for investigations into the potential applications of Hal3 in developing innovative therapeutic approaches targeting CoA metabolism-related disorders and diseases⁴³. Expanding upon previous research by Gerdes *et al.* (2002) and Spry *et al.* (2008), which investigated enzymes within the Coenzyme A (CoA) biosynthetic pathway as promising antimicrobial drug targets^{1,6}, this study underscores the importance of continued investigation in these domains. By delving deeper into the functional aspects of DhHal3p, researchers can glean invaluable insights crucial for the development of innovative antimicrobial agents. The study also underlines the value of homology modeling in predicting protein structures when atomic-level structures are unavailable. The predicted tertiary structure of DhHal3p offers insights into the structural basis of protein target specificity and ligand-binding mechanisms, serving as a blueprint for forthcoming experimental studies on this protein. The characterization of multifunctional enzymes from extremophilicholds significant potential for understanding and designing efficient metabolic pathways.

While this study is not exempt from limitations, such as the challenge of experimentally validating protein-ligand interactions due to resource constraints, it underscores the significance of future research endeavors. Specifically, employing alternative experimental techniques like gene knockouts or overexpression approaches is encouraged to validate these interactions. Further, the restricted availability of only a single template, the Phosphopantothenoylcysteine decarboxylase (also known as FMN binding protein AtHal3) from *A. thaliana* (PDB ID: 1E20), for DhHal3p poses a significant limitation. This template offers only 34% query coverage, 38.27% sequence identity, and a 1e-38 e-value against the target protein, potentially limiting the accuracy and comprehensiveness of structural predictions and requiring cautious interpretation of the results. Alternative interpretations of this study are DhHal3p might be forming homo or hexa-trimeric complex (as evident in native gel image) showing pyruvate decarboxylase

activity in contrast to heterotrimeric counterpart in *S. cerevisiae*. Moreover, pyruvate is not its reported substrate, so utilizing other known substrates may alter its activity and therefore conducting experiments with alternative substrates could provide valuable insights into the enzyme's substrate specificity and activity profile. To validate these findings, we should aim to characterize the oligomeric form of functional DhHal3p, determine its crystal structure, investigate its quaternary structure, and analyze its substrate specificity, as in⁴⁴. These efforts will enhance our understanding of DhHal3p's specific binding sites.

The future goal of this study would be to determine its crystal and quaternary structure and explore its substrate specificity and enzymatic activity in more detail. Genetic manipulation techniques, such as gene knockouts and overexpression, are essential for elucidating the functional significance of DhHal3p. Gene knockout experiments involving deleting or disrupting the DhHal3p gene in *D. hansenii*, could allow the researchers to assess the phenotypic consequences of DhHal3p loss-of-function. Conversely, gene overexpression experiments involve expressing additional copies of the DhHal3p into *D. hansenii*, which could enable researchers to evaluate the effects of DhHal3p overexpression on cellular processes and organismal physiology as indicated⁴⁵. Our future directions aimed towards unravelling the role of DhHal3p in a variety of cellular processes by adopting these techniques, paving the way for therapeutic interventions.

Conflict of interest

All authors declare no conflict of interest.

References

- 1 Spry C, Kirk K & Saliba KJ, Coenzyme A biosynthesis: an antimicrobial drug target. *FEMS Microbiol Rev*, 32 (2008) 56.
- 2 Albert A, Martínez-Ripoll M, Espinosa-Ruiz A, Yenush L, Culiáñez-Macià FA & Serrano R, The X-ray structure of the FMN-binding protein AtHal3 provides the structural basis for the activity of a regulatory subunit involved in signal transduction. *Structure*, 8 (2000) 961.
- 3 Kupke T, Hernández-Acosta P, Steinbacher S & Culiáñez-Macià FA, Arabidopsis thaliana Flavoprotein AtHAL3a Catalyzes the Decarboxylation of 4'-Phosphopantothenoylcysteine to 4'-Phosphopantetheine, a Key Step in Coenzyme A Biosynthesis. *J Biol Chem*, 276 (2001) 19190.
- 4 Steinbacher S, Hernández-Acosta P, Bieseler B, Blaesse M, Huber R & Culiáñez-Macià FA, Crystal Structure of the Plant PPC Decarboxylase AtHAL3a Complexed with an Ene-thiol Reaction Intermediate. *J Mol Biol*, 327 (2003) 193.

- 5 Ruiz A, González A, Muñoz I, Serrano R, Abrie JA & Strauss E, Moonlighting proteins Hal3 and Vhs3 form a heteromeric PPCDC with Ykl088w in yeast CoA biosynthesis. *Nat Chem Biol*, 5 (2009) 920.
- 6 Gerdes SY, Scholle MD, D'Souza M, Bernal A, Baev MV & Farrell M, From genetic footprinting to antimicrobial drug targets: examples in cofactor biosynthetic pathways. *J Bacteriol*, 184 (2002) 4555.
- 7 Posas F, Camps M & Ario J, The PPZ Protein Phosphatases Are Important Determinants of Salt Tolerance in Yeast Cells. *J Biol Chem*, 270 (1995) 13036.
- 8 Yenush L, Mulet JM, Ariño & Serrano R, The Ppz protein phosphatases are key regulators of K⁺ and pH homeostasis: implications for salt tolerance, cell wall integrity and cell cycle progression. *EMBO J*, 21 (2002) 920.
- 9 Vissi E, Clotet J, de Nadal E, Barceló A, Baó É, Gergely P, Dombrádi V & Ariño, Functional analysis of the Neurospora crassa PZL-1 protein phosphatase by expression in budding and fission yeast. *Yeast*, 18 (2001) 115.
- 10 Adám C, Erdei E, Casado C, Kovacs L, González A, Majoros L, Petrényi K, Bagossi P, Farkas I, Molnar M, Pócsi I, Ariño J & Dombrádi V, Protein phosphatase CaPpz1 is involved in cation homeostasis, cell wall integrity and virulence of *Candida albicans*. *Microbiology*, 158 (2012) 1258.
- 11 Minhas A, Sharma A, Kaur H, Rawal Y, Ganesan K & Mondal AK, Conserved Ser/Arg-rich motif in PPZ orthologs from fungi is important for its role in cation tolerance. *J Biol Chem*, 287 (2012) 7301.
- 12 Buzzini P & Martini A, Large-scale screening of selected *Candida maltosa*, *Debaryomyces hansenii* and *Pichia anomala* killer toxin activity against pathogenic yeasts. *Med Mycol*, 39 (2001) 479.
- 13 Medina-Córdova N, López-Aguilar R, Ascencio F, Castellanos T, Campa-Córdova AI & Angulo C, Biocontrol activity of the marine yeast *Debaryomyces hansenii* against phytopathogenic fungi and its ability to inhibit mycotoxins production in maize grain (*Zea mays* L.). *Biol Control*, 97 (2016) 70.
- 14 Ramos-Moreno L, Ruiz-Pérez F, Rodríguez-Castro E & Ramos J, *Debaryomyces hansenii* Is a Real Tool to Improve a Diversity of Characteristics in Sausages and Dry-Meat Products. *Microorganisms*, 9 (2021) 1512.
- 15 Minhas A, Biswas D & Mondal AK, Development of host and vector for high-efficiency transformation and gene disruption in *Debaryomyces hansenii*. *FEMS Yeast Res*, 9 (2009) 95.
- 16 Minhas A & Biswas D, Development of an efficient transformation system for halotolerant yeast *Debaryomyces hansenii* CBS767. *Bio-protocol*, 9 (2019) 3352.
- 17 Di Como CJ, Bose R & Arndt KT, Overexpression of SIS2, which contains an extremely acidic region, increases the expression of SWI4, CLN1 and CLN2 in *sit4* mutants. *Genetics*, 139 (1995) 95.
- 18 Duvaud S, Gabella C, Lisacek F, Stockinger H, Ioannidis V & Durinx C, ExPASy, the Swiss Bioinformatics Resource Portal, as designed by its users. *Nucleic Acids Res*, 49 (2021) 216.
- 19 Yates AD, Allen J, Amode RM, Azov AG, Barba M, Becerra A, Bhai J, Campbell LI, Martinez MC, Chakiachvili M, Chougule K, Christensen M, Contreras-Moreira B, Cuzick A, Fioretto, Paul LDR, Davis, De Silva NH, Diamantakis S, Dyer S, Elser J, Filippi CV, Gall A, Grigoriadis D, Guijarro-Clarke C, Gupta P, Hammond-Kosack KE, Howe KL, Jaiswal P, Kaikala V, Kumar V, Kumari S, Langridge N, Le T, Luypaert M, Maslen GL, Maurel T, Moore B, Matthieu Muffato, Mushtaq A, Naamati G, Naithani S, Olson A, Parker A, Paulini M, Pedro H, Perry E, Preece J, Quinton-Tulloch M, Rodgers F, Rosello M, Ruffier M, Seager J, Sitnik V, Szpak M, Tate J, Tello-Ruiz MK, Trevanion SJ, Urban M, Ware D, Wei S, Williams G, Winterbottom A, Zarowiecki M, Finn RD & Flicek P, Ensembl Genomes 2022: an expanding genome resource for non-vertebrates. *Nuc Acids Res*, 50 (2022) 996.
- 20 Bailey TL, Johnson J, Grant CE & Noble WS, The MEME Suite. *Nuc Acids Res*, 43 (2015) 39.
- 21 Kumar S, Stecher G, Li M, Knyaz C & Tamura K, MEGA X: Molecular Evolutionary Genetics Analysis across Computing Platforms. *Mol Biol Evol*, 35 (2018) 1547.
- 22 Wang Y, Xiao J, Suzek TO, Zhang J, Wang J & Bryant SH, PubChem: a public information system for analyzing bioactivities of small molecules. *Nuc Acids Res*, 37 (2009) 623.
- 23 Webb B & Sali A, Comparative protein structure modeling using MODELLER. *Curr Protoc Bioinforma*, 54 (2016) 1.
- 24 Altschul SF, Gish W, Miller W, Myers EW & Lipman DJ, Basic local alignment search tool. *J Mol Biol*, 215 (1990) 403.
- 25 Krieger E, Joo K, Lee J, Lee J, Raman S, Thompson J, Baker D & Karplus K, Improving physical realism, stereochemistry, and side-chain accuracy in homology modeling: Four approaches that performed well in CASP8. *Proteins Struct Funct Bioinforma*, 77 (2009) 114.
- 26 Hanwell MD, Curtis DE, Lonie DC, Vandermeersch T, Zurek E & Hutchison GR, Avogadro: An advanced semantic chemical editor, visualization, and analysis platform. *J Cheminform*, 4 (2012).
- 27 Morris GM, Ruth H, Lindstrom W, Sanner MF, Belew RK, Goodsell DS & Olson AJ, AutoDock4 and AutoDockTools4: Automated docking with selective receptor flexibility. *J Comput Chem*, 30 (2009) 2785.
- 28 Burke D & Dawson D, No Title. *Cold Spring Harbor Laboratory Press*, (2000).
- 29 Wood EJ, Molecular cloning: A laboratory manual. *Biochem Educ*, 11 (1983) 82.
- 30 Hefti MH, Vervoort J & van Berkel WJH, Defflavination and reconstitution of flavoproteins. *Eur J Biochem*, 270 (2003) 4227.
- 31 Gounaris AD, Turkenkopf I, Buckwald S & Young A, Pyruvate Decarboxylase: I. Protein dissociation into subunits under conditions in which thiamine pyrophosphate is released. *J Biol Chem*, 246 (1971) 1302.
- 32 Espinosa-Ruiz A, Bellés JM, Serrano R & Culiáñez-Macià FA, Arabidopsis thaliana AtHAL3: a flavoprotein related to salt and osmotic tolerance and plant growth. *Plant J*, 20 (1999) 529.
- 33 Kupke T, Stevanovic S, Sahl H & Götz F, Purification and Characterization of Epid, a Flavoprotein Involved in the Biosynthesis of the Lantibiotic Epidermin. *J Bacteriol*, 174 (1992) 5354.
- 34 Majer F, Schmid DG, Altena K, Bierbaum G & Kupke T, The flavoprotein MrsD catalyzes the oxidative decarboxylation reaction involved in formation of the peptidoglycan biosynthesis inhibitor mersacidin. *J Bacteriol*, 184 (2002) 1234.

- 35 Spitzer ED & Weiss B, dfp Gene of *Escherichia coli* K-12, a locus affecting DNA synthesis, codes for a flavoprotein. *J Bacteriol*, 164 (1985) 994.
- 36 Agarwal PK, Uppada V & Noronha SB, Comparison of pyruvate decarboxylases from *Saccharomyces cerevisiae* and *Komagataella pastoris* (*Pichia pastoris*). *Appl Microbiol Biotechnol*, 97 (2013) 9439.
- 37 Kikani BA & Singh SP, Enzyme stability, thermodynamics and secondary structures of α -amylase as probed by the CD spectroscopy. *Int J Biol Macromol*, 81 (2015) 450.
- 38 Benjamin W & Andrej S, Comparative protein structure modeling using modeller. *Curr Protoc Bioinforma*, 54 (2016) 1.
- 39 Nambiar MP, Jayadevan S, Babu BK & Biju AR, Computational studies on the structural variations of MAO-A and MAO-B inhibitors - An *in silico* docking approach. *Indian J Biochem Biophys*, 59 (2022) 276.
- 40 Agrawal A, T Kulkarni G & Lakshmayya, Molecular docking study to elucidate the anti-pruritic mechanism of selected natural ligands by desensitizing TRPV3 ion channel in Psoriasis: An *in silico* approach. *Indian J Biochem Biophys*, 57 (2020) 578.
- 41 Kumar A, Mishra T & Kulshreshtha A, Binding interaction of laccases from *Bacillus Subtilis* after industrial dyes exposure: Molecular docking and molecular dynamics simulation studies. *Indian J Biochem Biophys*, 60 (2023) 320.
- 42 Petrényi K, Molero C, Kónya Z, Erdődi F, Ariño J & Dombrádi V, Analysis of Two Putative *Candida albicans* Phosphopantothenoylcysteine Decarboxylase / Protein Phosphatase Z Regulatory Subunits Reveals an Unexpected Distribution of Functional Roles. *PLoS One*, 11 (2016) e0160965.
- 43 Cavestro C, Diodato D, Tiranti V & Di Meo I, Inherited Disorders of Coenzyme A Biosynthesis: Models, Mechanisms, and Treatments. *Int J Mol Sci*, 24 (2023) 5951.
- 44 Kaur R, Sharma S, Kaur S & Sodhi HS, Biochemical characterization with kinetic studies of melanogenic enzyme tyrosinase from white button mushroom, *Agaricus bisporus*. *Indian J Biochem Biophys*, 59 (2022) 718.
- 45 Bhuvanasundar R, Ragavachetty NN, Singh NK, Coral K, Deepa PR & Sulochan KN, Expression, purification and characterization of a biologically active and thermally stable human lysyl oxidase. *Indian J Biochem Biophys*, 56 (2019) 105.